Unipolar half-cycle pulse generation in asymmetrical media with a periodic subwavelength structure

Xiaohong Song,[*] Weifeng Yang,[†] Zhinan Zeng, Ruxin Li, and Zhizhan Xu[‡]
State Key Laboratory of High Field Laser Physics, Shanghai Institute of Optics and Fine Mechanics, Chinese Academy of Sciences, Shanghai 201800, China
(Received 11 June 2010; published 17 November 2010)

We present a method to generate an extremely short unipolar half-cycle pulse based on resonant propagation of a few-cycle pulse through asymmetrical media with periodic subwavelength structure. Moreover, single- and few-cycle gap solitons with different frequencies are found to split from one incident few-cycle ultrashort pulse. These solitons with various frequencies provide evidence for the generation of different parametric waves during the strong light-matter coupling in asymmetrical media under the extreme nonlinear optics condition. Because of the pulse self-shaping process during the course of resonant propagation, the generated low-frequency sideband and another broadband continuum sideband ranging from the visible to the near-infrared regime couple together, which results in the generation of the subfemtosecond unipolar half-cycle pulse. A time-frequency analysis is preformed which corroborates the mechanism. The generated unipolar half-cycle pulse might be utilized to control and probe the ultrafast electronic dynamics.

DOI: 10.1103/PhysRevA.82.053821 PACS number(s): 42.65.Re, 42.50.Md

I. INTRODUCTION

Generation and synthesis of single and subcycle pulses have attracted considerable interest since such pulses have great potential for application in many areas such as attosecond pulse generation and ultrafast control of electronic dynamics [1–3]. Compared with oscillating few- or single-cycle pulses, the unipolar half-cycle pulse has a unique feature, that is, unidirectionality. When the duration (T_p) is much shorter than the electron classical orbital period ($T_n \approx 2\pi n^3$ a.u.), the half-cycle pulse effectively delivers an impulsive momentum transfer or kick to the electron [4–7]. This behavior can be used to control and detect the dynamics of the wave packet [4–7]. The now-available half-cycle pulses are mainly in the tetrahertz frequency region, with pulse duration of hundreds of femtoseconds [8,9]. Such half-cycle pulses reach the requirement $T_p \ll T_n$ only for Rydberg states with large principal quantum number n. Subpicoseond half-cycle tetrahertz pulses have been widely used as tools to control and view Rydberg electron dynamics during the last few years [4–7]. To extend this electronic wave packet control-probe scheme to low excited states, extremely short (on the subfemtosecond or attosecond time scale) half-cycle pulses are needed. As a result, generation of single or trains of subfemtosecond half-cycle pulses in the visible or near-infrared region will be of particular significance [10].

Recently, it has been suggested that the resonant propagation of a few-cycle ultrashort laser pulse in nonlinear media might be a promising candidate for shortening ultrashort laser pulses to single or even subcycle pulse durations [11,12]. The resonant strong interaction of the laser pulse with matter is one of the most striking effects of nonlinear optics. It gives rise to many novel effects such as self-induced transparency [13,14], pulse splitting [13,15], and Rabi oscillation [13,16–20]. The carrier-envelope phase (CEP)-dependent resonant strong interaction also provides routines to measure the CEP of few-cycle ultrashort laser pulses with moderate intensities [21–24]. When the violation of the inversion symmetry of a two-level system is considered, recent investigation has demonstrated that the Rabi oscillations are manifest in the frequency domain as a new singlet Rabi sideband at the Rabi frequency Ω as well as the well-known Mollow triplets with frequencies $n\omega_p \pm \Omega$ [25].

Here we present a method, based on both the resonant propagation effects and violation of the inversion symmetry of the medium, to generate extremely short unipolar half-cycle pulses in the optical frequency range. The idea is that when a two-level system with broken inversion symmetry is exposed to a few-cycle ultrashort laser pulse, broadband Rabi sidebands at frequencies $\tilde{\Omega}(t)$ and $n\omega_p \pm \tilde{\Omega}(t)$ will occur (here $\tilde{\Omega}(t) = \mu_{12}\tilde{E}(t)/\hbar$ is the time-dependent Rabi frequency and $\tilde{E}(t)$ is the time-dependent electric field envelope amplitude). During the course of the resonant propagation, the transient emission of the system will lead to energy redistributions in the propagating pulse, which will result in pulse deformation. Our results show, very interestingly, that this resonant analog of the self-shaping process can result in the coherent superposition of the generated low-frequency component and another broadband continuum spectrum in the optical frequency regime, which is expected to synthesize an extremely short unipolar pulse. Moreover, solitons with different frequencies can be achieved simultaneously. These phenomena provide a new route to pulse shaping and compression.

II. THEORETICAL APPROACH

We adopt a period structure because it has been demonstrated that subwavelength structure can be used to suppress the intrapulse four-wave mixing in continuous media [12]. As a result, the evolutions and the interactions among different Rabi sideband components inherent in asymmetrical media can be clearly shown. Moreover, a period array of thin

[*]Present address: Department Physik and Center for Optoelectronics and Photonics Paderborn (CeOPP), Universität Paderborn, Warburger Str. 100, D-33098 Paderborn, Germany.
[†]wfeng_yang@yahoo.com.cn; Present address: Arnold Sommerfeld Center for Theoretical Physics, Ludwig-Maximilians-Universität München, Theresienstraße 37, 80333 München, Germany.
[‡]zzxu@mail.shcnc.ac.cn

layers of resonant two-level system reveals an example of an artificial medium which has attracted great attention in recent years [12,26]. As for the asymmetrical two-level systems, various different types of candidates for media, such as the artificial low-dimension structures (quantum dot, wells, wire), polar molecules, and atoms imposed onto a static electric field, among others, have been discussed in detail in Refs. [25,27–31].

The critical parameter which distinguishes the asymmetrical two-level systems from the symmetrical ones is the nonzero difference between the permanent dipole moments (PDMs) $d = \mu_{22} - \mu_{11}$, where μ_{ij} are the dipole moment matrix elements. When the violation of the inversion symmetry is considered, the full-wave Maxwell-Bloch equations beyond the slowly varying envelope approximation and rotating wave approximation can be written as follows:

$$\frac{\partial H(z,t)}{\partial t} = -\frac{1}{\mu_0}\frac{\partial E(z,t)}{\partial z},$$
$$\frac{\partial E(z,t)}{\partial t} = -\frac{1}{\varepsilon_0}\frac{\partial H(z,t)}{\partial z} - \frac{\omega_c(z)}{\varepsilon_0}\frac{\partial P(z,t)}{\partial t}, \tag{1}$$

$$\dot{u} = -\omega_0 v + \frac{d}{\hbar}E(t)v - \frac{1}{T_2}u,$$
$$\dot{v} = \omega_0 u + 2\frac{\mu_{12}}{\hbar}E(t)w - \frac{d}{\hbar}E(t)u - \frac{1}{T_2}v, \tag{2}$$
$$\dot{w} = -2\frac{\mu_{12}}{\hbar}E(t)v - \frac{1}{T_1}(w+1).$$

Here H, P, μ_0, and ε_0 are the magnetic field, the macroscopic polarization, the permeability, and the permittivity of free space, respectively. $P = NTr(\rho\mu), \rho$ is the density matrix. The initial field with a hyperbolic secant shape is defined as $E(t) = \tilde{E}(t)\cos[\omega_p(t-t_0)] = E_0 \sec h[(t-t_0)/\tau_0]\cos[\omega_p(t-t_0)]$, where ω_p is the central frequency and $\tau_p = 2ar\cosh(1/\sqrt{0.5})\tau_0$ is the full width at half maximum (FWHM) of the pulse envelope. The envelope area of the pulse is determined by $A(z,t=0) = (\mu_{12}/\hbar)\int_{-\infty}^{\infty}\tilde{E}(z,t')dt' = (\mu_{21}E_0\tau_p\pi)/1.76\hbar$, where ω_0 is the resonant frequency and T_1 and T_2 are, respectively, the lifetime of the excited state and the dephasing time. We define the dimensionless variable $r = d/\mu_{12}$, which denotes the asymmetry parameter of the medium. This parameter can be much different for various media, for example, it has the magnitude $r \sim 1.0$ for some III-nitride quantum dots [25], $r \sim 2.2$ for some substituted aromatic molecules [27,28], and $r \sim 0.4$–14.0 for some types of semiconductor wells [29,30]. To investigate the role of violation of the inversion symmetry in the propagation effect, we consider a one-dimensional periodic structure similar to that in Ref. [12] but for various nonzero asymmetry parameters r. The parameters are as follows [12]: $\tau_p = 5$ fs, $\omega_p = \omega_0 = 2.3\,\text{fs}^{-1}$ (corresponding to $\lambda_0 = 830$ nm), $\mu_{12} = 2\times10^{-29}$ Asm, $T_1 = 1$ ps, $T_2 = 0.5$ ps, the density of the resonant medium $N = 4.4\times10^{20}$ cm^{-30}. The pulse area A $= 1\pi$ corresponds to a maximum electric-field amplitude $E_0 = 1.856\times10^7$ V/cm or an intensity of $I = 1.33\times10^{-3}$, $E_0^2 = 4.58\times10^{11}$ W/cm^2. The peak Rabi frequency $\Omega_0 = 2.1$ fs^{-1} corresponds to an input envelope area A $= 6\pi$. It has been demonstrated that under the extreme nonlinear regime, a two-level system can be still used to reproduce the experimental results amazingly well [16,22,23]. We consider a tight periodic structure with same thicknesses ($\delta = 0.1$, $\lambda_0 = 83$ nm) of the thin layer of asymmetrical two-level systems and the transparent material which separates the films because for tighter periodic structure, more energy of the incident pulse is located in the penetrating part [12] on which we concentrate. The full-wave Maxwell-Bloch equations are numerically solved by using the finite-difference-time-domain method. This method has proven to be an accurate ab initio tool to simulate the interaction between few-cycle ultrashort pulses and matter [11,12,14–17,21–24].

III. NUMERICAL RESULTS

Figures 1(a) and 1(b) show the electric-field profiles of the pulse before and after propagation through the asymmetrical resonant period structure, respectively. It can be seen that the incident pulse splits into several pulses, including both near-single-cycle and few-cycle gap soliton pulses. Most strikingly, a unipolar half-cycle pulse with a FWHM about 0.5 fs (500 as) can be generated, and the amplitude is even higher than those of the generated few- and near-single-cycle pulses. To see clearly the frequency contents of the generated pulses, we perform time-frequency analysis by means of the wavelet transform of the transmitted electric field [32,33] [see Fig. 1(c)]. The time-frequency analysis can map out the instantaneous spectral amplitude as a function of both time and frequency. Compared to the conventional spectrum, the 3-D time-frequency analysis graph can clearly show the details of the spectral structures at different part of the electric field, thus helping us understand the underlying physical processes [20,34].

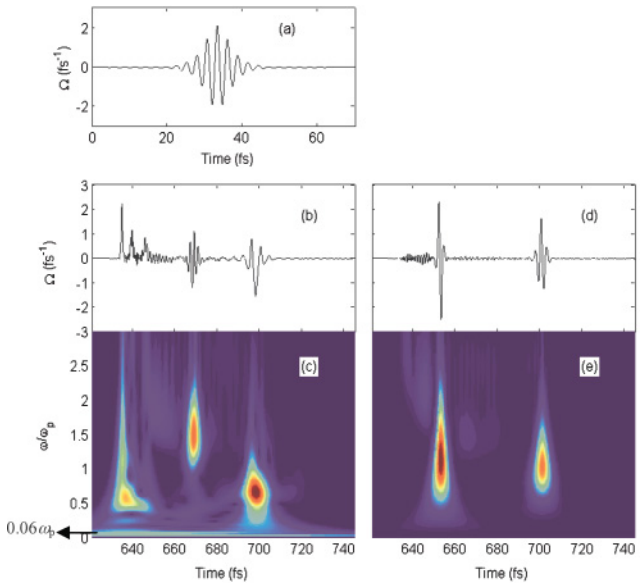

FIG. 1. (Color online) (a) The initial incident few-cycle ultrashort pulse. (b, c) The temporal shape of the electric field outside the periodic structure and the corresponding time-frequency analysis graph for $r = 2.0$. (d, e) As in (b) and (c), but for $r = 0.0$. The length of the period structure $L = 160$ μm, and the input and output interfaces of the periodic structure are at $z = 20$ μm and $z = 186$ μm, respectively.

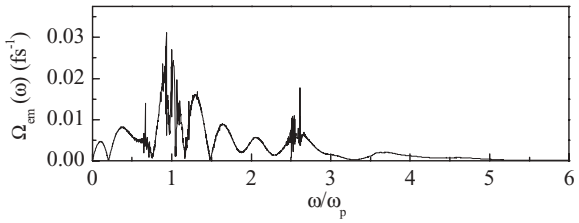

FIG. 2. The spectrum of the reemitted field near the input face $z = 20.04\ \mu$m, i.e., in the first subwavelength film.

Several distinct features are noticed from the electric field profiles [Fig. 1(b)] and the corresponding time-frequency analysis graph [Fig. 1(c)]. First, the generated unipolar half-cycle pulse is mainly composed of two frequency components: One is a broad continuum spectrum from $0.5\omega_p$ to $3.0\omega_p$ (i.e., wavelength λ from about 1660 to 270 nm) and the other is the low-frequency component at around $0.06\omega_p$ (i.e., $\lambda \approx 14\ \mu$m, indicated by the arrow). Moreover, interference patterns can be seen between these two spectral components. To explore the root of the unipolar half-cycle pulse generation, as a comparison, we further calculate the case of a few-cycle pulse propagation in a symmetrical period structure with parameters the same as in Figs. 1(b) and 1(c), except for $r = 0$ [see Figs. 1(d) and 1(e)]. No low-frequency component occurs in the time-frequency analysis graph, and neither does the unipolar half-cycle pulse in the transmitted pulses in this case, which is consistent with what was predicted in Ref. [12]. As a result, the low-frequency components generated in the nonzero PDM system play a key role in the generation of the unipolar half-cycle pulse. Second, in contrast with the symmetrical system case [Fig. 1(e)], in which the penetrating spectra are situated around the input central frequency ω_p, both blueshift and redshift occur simultaneously in the transmitted pulses when the inversion symmetry of the system is broken. The frequencies of the generated gap solitons are different with central frequencies at about 1.5 ω_p (i.e., $\lambda \approx 550$ nm) and 0.6 ω_p (i.e., $\lambda \approx 1380$ nm), respectively, which means solitons with different frequencies can be split from one incident few-cycle ultrashort pulse.

To explore how these unique pulses are formed, we present in Fig. 2 the spectrum of the reemitted field at the first subwavelength film. The reemitted field is proportional to the time derivative of the macroscopic polarization, that is, $E_{em}(t) \propto -\partial P_x/\partial t$ [21,35], which reflects directly the transient response of the medium to the field. Different from the cw field case predicted in Ref. [25], there, the radiation spectrum consists of a distinct singlet at frequency Ω_0 and an infinite sequence of triplets with a frequency sequence of triplets with $n\omega_p \pm \Omega_0$. In our case, the radiation spectrum is a quasicontinuum from 0 to 5 ω_p, with an obvious interference pattern. The reason is that (1) since the Rabi sidebands occur at frequency $\tilde{\Omega}(t)$ and $n\omega_p \pm \tilde{\Omega}(t)$ for the pulse case in asymmetrical system, the frequency span of each sideband is from 0 to Ω_0 and from $n\omega_p - \Omega_0$ to $n\omega_p + \Omega_0$, respectively. When the few-cycle ultrashort laser pulse excitation is considered, the high temporal gradient of the pulse allows broadband Rabi shifting, and different broadband Rabi sidebands can even meet each other [16,17,22,23]. (2) Also, the Rabi frequencies reach the same values at both the leading part and the tail part of the pulse and result in the same sideband frequencies; the interference between them creates the periodic pattern in the reemission spectrum.

During the course of pulse propagation, the macroscopic polarization built in the medium will act as a source of the reemitted field, which will affect the propagating pulse, and pulse deformation can be appreciable. According to the famous area theorem [13], the basic physical process of pulse propagation in a resonant medium is that the medium absorbs photons from the pulse and excites electrons from the ground state to the excited state, and then emits them back to the pulse when the electrons return to their ground state. Through exchanging energy with the medium, the input pulse gets deformed and stabilizes, eventually, into a certain form. This energy exchange is the root of pulse split and other deformation during the course of resonant propagation [13]. In our case, since there are Rabi sidebands with difference frequencies, this pulse self-shaping process will induce the coupling of the generated low-frequency component and the other broadband continuum spectrum, which will further result in the generation of the unipolar subfemtosecond ultrashort half-cycle pulse.

The process of pulse shaping can be clearly seen in Fig. 3, which shows the evolution of the penetrating pulse and the

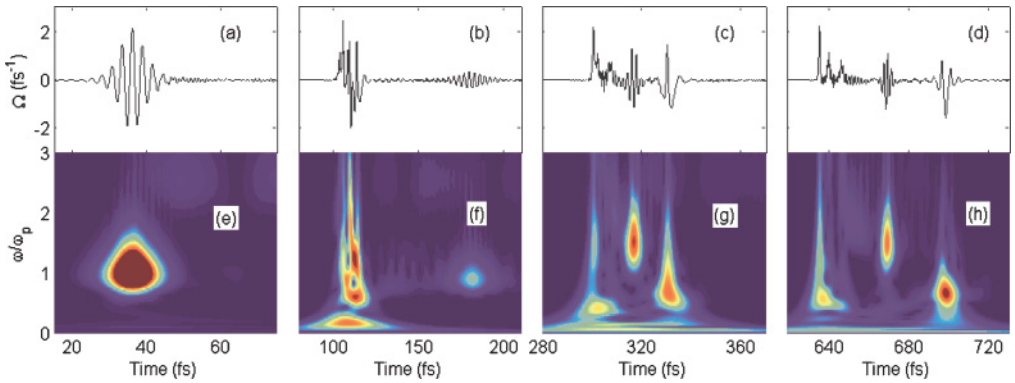

FIG. 3. (Color online) (top) Evolution of the pulse and (bottom) the corresponding the time-frequency analysis graphs during propagation inside and outside the period structure for (a) $r = 2.0$ and (e) $z = 20.04\ \mu$m, i.e., in the first layer film; (b, f) $z = 41.57\ \mu$m, i.e., in the 261st layer film; (c, g) $z = 99.64\ \mu$m, i.e., in the 987th layer film; and (d, h) $z = 200\ \mu$m, i.e., outside the periodic structure.

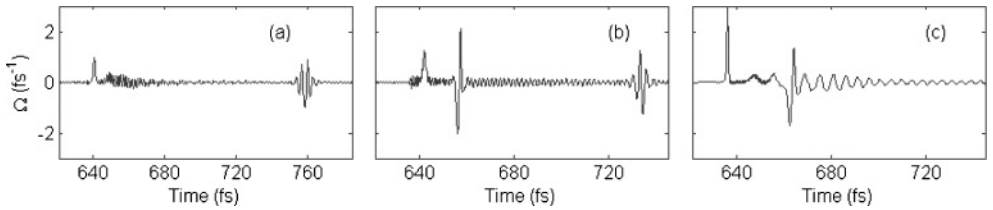

FIG. 4. (a) As in Fig. 1(b), but for the $A = 4\pi$ case. (b) As in Fig. 1(b), but for the $r = 1.0$ case. (c) As in Fig. 4(b), but for the two-photon resonant ($\omega_p = \omega_0/2$) case.

corresponding time-frequency analysis graphs during propagation through the periodic structure. As can be observed, near the input face (i.e., in the first film), the impact of the transient response of the medium on the propagating pulse is very small. While after some propagation distance, the pulse deformation can be obviously appreciable, one soliton pulse is split from the main part. The corresponding time-frequency analysis graph [Fig. 3(f)] shows that the frequency of the generated soliton pulse is equal to the transition frequency of the medium. Owing to the slower velocity of the soliton, it falls quickly behind the main pulse. The spectral composition of the main pulse is very complicated, including both a low-frequency component located around 0.2 ω_p and a quasicontinuum spectrum ranging from 0.5 ω_p to 3 ω_p. With further propagation, the main part of the pulse will split into several pulses with different frequencies [see Figs. 3(c) and 3(g)]. In the leading part of the electric field, the low-frequency component and the quasicontinuum spectrum have comparable intensity. Their combination forms the unipolar characteristic of the electric field [see Figs. 3(b), 3(c), 3(f), and 3(g)]. This part of the electric field will further evolve into a unipolar half-cycle pulse [see Figs. 3(c) and 3(d)], while the lower frequency components contained in the generated few- and single-cycle pulses are much weaker than the other frequency components, so their influence on the pulse shape is relatively small [see Figs. 3(c), 3(d), 3(f), and 3(g)]. Once these pulses are formed, they can maintain their envelope shape for a long propagation distance, despite that their phases are changing [see Figs. 3(c) and 3(d)], which is a typical behavior of the gap soliton in periodic structure [12].

There are several ways to control the intensity of the unipolar half-cycle pulse: first, by controlling the incident laser pulse intensity; second, using different asymmetrical media. This is because the intensity of the generated low-frequency component depends on both the driving field E and the magnitude of the PDM: $I_R \propto d^2\Omega^4$ (see Ref. [25]). Third, one can also adopt different resonant conditions: $\omega_p = \omega_0/m$ ($m = 1,2,3\ldots$). This is because, according to the prediction by the analytical analysis in Ref. [25], when m is increased, the amplitude of Rabi sidebands at frequency $n\omega_p \pm \tilde{\Omega}(t)$ will decrease, while the low-frequency sidebands at frequency $\tilde{\Omega}(t)$ are unaffected, which will decrease the energy splitting from the main pulse and thus keep more energy in the main pulse so as to increase the intensity of the generated unipolar half-cycle pulse. Figure 4 shows the temporal shape of the transmitted pulse for various cases. It can be seen that both decreasing the amplitude of the incident pulse and using an asymmetrical medium with smaller r can decrease the amplitude of the generated unipolar half-cycle pulse [see Figs. 1(b), 4(a), and 4(b)], while for the two-photon resonant case, the generated unipolar half-cycle pulse will become much stronger even for the small r ($r = 1.0$) case [see Figs. 4(a) and 4(c)]. Our numerical calculation results further confirm the preceding analysis. It should be emphasized that the frequency multiplication, especially the low-frequency component generation, is the general property inherent to the systems with broken inversion symmetry, and pulse splitting and shaping is also a common phenomenon of resonant propagation in both the continuous and period structures. Moreover, it has been demonstrated that even when the electronic dispersion and multitude of other resonance transitions are considered [17], the two-level system can still be used to simulate the sidebands' effects in some semiconductor nanostructures which are the base of the generation of the extremely short unipolar half-cycle pulse in our work. Consequently, the results presented in this article are expected to manifest in different quantum systems with nonzero permanent dipole moments.

IV. CONCLUSION

In summary, we have introduced a new method to generate extremely short unipolar half-cycle pulses in the optical frequency regime based on the self-shaping of few-cycle ultrashort lasers during the course of resonant propagation in asymmetrical media with a periodic subwavelength structure. The process of this self-shaping of few-cycle pulses includes a superposition of a low-frequency component and a broadband continuum spectrum in the optical frequency regime, which constructs the unipolar half-cycle pulse. The 3-D time-frequency analysis shows clearly the evolution and the underlying physical processes. The proposed scheme might be helpful for extremely short pulse shaping and compression, which have wide application potential in attosecond science and extremely nonlinear optics.

ACKNOWLEDGMENTS

The work was supported by the National Basic Research Program of China (Grant No. 2006CB806000 and No. 2010CB923203) and by the National Natural Science Foundation of China (Grant No. 60808008). W.Y. was also sponsored by the Shanghai Rising-Star Program (Grant No. 08QA14072).

[1] E. Goulielmakis *et al.*, Science **320**, 1614 (2008).

[2] G. Krauss, S. Lohss, T. Hanke, A. Sell, S. Eggert, R. Huber, and A. Leitenstorfer, Nature Photon. **4**, 33 (2010).

[3] T. Brabec and F. Krausz, Rev. Mod. Phys. **72**, 545 (2000); A. Nazarkin and G. Korn, Phys. Rev. Lett. **83**, 4748 (1999); Phys. Rev. A **58**, R61 (1998).

[4] J. J. Mestayer, W. Zhao, J. C. Lancaster, F. B. Dunning, C. O. Reinhold, S. Yoshida, and J. Burgdörfer, Phys. Rev. Lett. **99**, 183003 (2007).

[5] J. G. Zeibel and R. R. Jones, Phys. Rev. Lett. **89**, 093204 (2002).

[6] R. R. Jones, D. You, and P. H. Bucksbaum, Phys. Rev. Lett. **70**, 1236 (1993).

[7] C. Wesdorp, F. Robicheaux, and L. D. Noordam, Phys. Rev. Lett. **87**, 083001 (2001).

[8] Y. Gao, T. Drake, Z. Chen, and M. F. DeCamp, Opt. Lett. **33**, 2776 (2008).

[9] B. I. Greene, J. F. Federici, D. R. Dykaar, R. R. Jones, and P. H. Bucksbaum, Appl. Phys. Lett. **59**, 893 (1991).

[10] E. Persson, K. Schiessl, A. Scrinzi, and J. Burgdörfer, Phys. Rev. A **74**, 013818 (2006); A. Emmanouilidou and T. Uzer, *ibid.* **77**, 063416 (2008); J. S. Briggs and D. Dimitrovski, New J. Phys. **10**, 025013 (2008).

[11] V. P. Kalosha and J. Herrmann, Phys. Rev. Lett. **83**, 544 (1999).

[12] X. T. Xie and M. A. Macovei, Phys. Rev. Lett. **104**, 073902 (2010).

[13] Y. R. Shen, *The Principles of Nonlinear Optics* (Wiley, New York, 1984); L. Allen and J. H. Eberly, *Optical Resonance and Two-Level Atoms* (Wiley, New York, 1975); S. L. McCall and E. L. Hahn, Phys. Rev. Lett. **18**, 908 (1967).

[14] R. W. Ziolkowski, J. M. Arnold, and D. M. Gogny, Phys. Rev. A **52**, 3082 (1995).

[15] S. Hughes, Phys. Rev. Lett. **81**, 3363 (1998).

[16] T. Udem, Nature (London) **420**, 469 (2002); O. D. Mücke, T. Tritschler, M. Wegener, U. Morgner, and F. X. Kärtner, Phys. Rev. Lett. **87**, 057401 (2001); Opt. Lett. **27**, 2127 (2002); T. Tritschler, O. D. Mücke, and M. Wegener, Phys. Rev. A **68**, 033404 (2003).

[17] D. Golde, T. Meier, and S. W. Koch, J. Opt. Soc. Am. B **23**, 2559 (2006).

[18] Q. T. Vu, H. Haug, O. D. Mücke, T. Tritschler, M. Wegener, G. Khitrova, and H. M. Gibbs, Phys. Rev. Lett. **92**, 217403 (2004).

[19] R. Compton, A. Filin, D. A. Romanov, and R. J. Levis, Phys. Rev. Lett. **103**, 205001 (2009).

[20] G. Günter *et al.*, Nature (London) **458**, 178 (2009).

[21] W. F. Yang, X. H. Song, S. Q. Gong, Y. Cheng, and Z. Z. Xu, Phys. Rev. Lett. **99**, 133602 (2007).

[22] O. D. Mücke, T. Tritschler, M. Wegener, U. Morgner, and F. X. Kärtner, Phys. Rev. Lett. **89**, 127401 (2002).

[23] M. Wegener, *Extreme Nonlinear Optics* (Springer, Berlin, 2005); O. D. Mücke, T. Tritschler, and M. Wegener, Top. Appl. Phys. **95**, 379 (2004).

[24] C. Van Vlack and S. Hughes, Phys. Rev. Lett. **98**, 167404 (2007).

[25] O. V. Kibis, G. Y. Slepyan, S. A. Maksimenko, and A. Hoffmann, Phys. Rev. Lett. **102**, 023601 (2009).

[26] A. Kozhekin and G. Kurizki, Phys. Rev. Lett. **74**, 5020 (1995).

[27] R. Bavli, D. F. Heller, and Y. B. Band, Phys. Rev. A **41**, 3960 (1990).

[28] M. A. Kmetic, R. A. Thuraisingham, and W. J. Meath, Phys. Rev. A **33**, 1688 (1986).

[29] S. O. Elyutin, J. Phys. B **40**, 2533 (2007).

[30] S. Koinac, Z. Ikonić, and V. Milanović, Opt. Commun. **140**, 89 (1997).

[31] M. Drobizhev, F. Q. Meng, A. Rebane, Y. Stepanenko, E. Nickel, and C. W. Spangler, J. Phys. Chem. B **110**, 9802 (2006).

[32] X. M. Tong and S. I. Chu, Phys. Rev. A **61**, 021802(R) (2000).

[33] C. K. Chui, *An Introduction to Wavelets* (Academic, New York, 1992).

[34] W. F. Yang, X. H. Song, Z. N. Zeng, R. X. Li, and Z. Z. Xu, Opt. Express **18**, 2558 (2010).

[35] C. W. Luo, K. Reimann, M. Woerner, T. Elsaesser, R. Hey, and K. H. Ploog, Phys. Rev. Lett. **92**, 047402 (2004).